Supporting Information

Alkyne-Functionalized Ruthenium Nanoparticles: Impact of Metal-Ligand Interfacial Bonding Interactions on the Selective Hydrogenation of Styrene

Fengqi Zhang[†,a] Jingjing Fang[†,a] Lin Huang[†,a] Wenming Sun,[b] Zhang Lin,[c] Zhenqing Shi [c], Xiongwu Kang*[a] and Shaowei Chen*[a,d]

[a] Guangzhou Key Laboratory for Surface Chemistry of Energy Materials, New Energy Research Institute, School of Environment and Energy, South China University of Technology, Guangzhou Higher Education Mega Centre, Guangzhou 510006, China

[b] State Key Laboratory of Green Building Materials, China Building Materials Academy, Beijing 100041, China

[c] Guangdong Engineering and Technology Research Center for Environmental Nanomaterials, School of Environment and Energy, South China University of Technology, Guangzhou, Guangdong 510006, China

[d] Department of Chemistry and Biochemistry, University of California, 1156 High Street, Santa Cruz, California 95064, United States

* E-mails: esxkang@scut.edu.cn; shaowei@ucsc.edu

Experimental Section

Synthesis of 1,4-bis(4-hexylphenyl)buta-1,3-diyne (DEHB)

1,4-bis(4-hexylphenyl)buta-1,3-diyne was prepared by following a reported procedure.[1] N,N,N',N'-tetramethylethylenediamine (41.4 µl, 276 µmol, 20 mol%) and triethylamine (574 µl, 4.14 mmol, 3.0 eq) were added to THF (2.6 ml). Then 1-bromo-4-ethynylbenzene (250 mg, 1.38 mmol, 1.0 eq), $NiCl_2 \cdot 6\ H_2O$ (19.8 mg, 69.1 µmol, 5 mol%) and copper iodide (13.2 mg, 69.1 µmol, 5 mol%) were added. The reaction mixture was stirred at room temperature for 20 h, whereupon the solvent was removed under reduced pressure. The crude product was purified by column chromatography (silica gel, petroleum ether/dichloromethane 1:1) to obtain a colorless solid (212 mg, 589 µmol, 85%).

Synthesis of 1,2-bis(4-hexylphenyl) ethyne (BEHB)

1,2-bis(4-hexylphenyl) ethyne was prepared by following a reported procedure.[2] 1-bromo-4-hexyl-benzene(3 mmol, 720 mg),1-ethnyl-hexylbenzene(3.3 mol, 614.3 mg) was added into a round-bottom flask. Then bis(triphenylphosphine)-palladium(II) chloride (0.02 eq, 0.06 mmol) and CuI(0.04 eq, 0.12 mmol) was added slowly. Finally, the triethylamine was added into the mixture solvents and the reaction was allowed to stir for 2 hours at room temperature. At the same time, the color of solvents became colorless to dark. And the solvent was removed under reduced pressure. The crude product was purified by column chromatography (silica gel, hexane/ dichloromethane 1:1) to obtain a colorless solid (453 mg, 1.31 mol, 63%).

Preparation of ruthenium nanoparticles

Ru nanoparticles were synthesized by thermal-reduction of $RuCl_3$ in 1,2-propanediol. Briefly, “bare” ruthenium colloids were synthesized by thermal refluxing of 0.28 mmol $RuCl_3$ and 2 mmol sodium actetate in 1,2-propanediol (100 mL) at 165 °C for 30 min under vigorous stirring. When the solution was cooled down to room temperature, 0.84 mmol of EHB was added into the

above solution with 100 mL toluene. An intense color appearance in the toluene phase was observed whereas the propanediol phase became colorless, indicating the successful extraction of the particles from the propanediol phase to the toluene phase, as a result of self-assembly of alkynes onto the nanoparticles surface. The toluene phase was collected and dried by rotary evaporation. The solids were then rinsed with a copious amount of methanol to remove excessive ligands. The resulting nanoparticles were denoted as Ru@EHB. Ruthenium nanoparticles passivated by DEPy, BEHB, DEHB, phenylethanethiol (PThiol) and 1-dodecyne were prepared in a similar fashion and the corresponding nanoparticles were defined as Ru@DEPy, Ru@BEHB, Ru@DEHB, Ru@PThiol and Ru@HC12.[3]

Hydrogenation of styrene

Ruthenium nanoparticles were dispersed in THF inside a Fischer Porter bottle, along with 1 mL of styrene. The bottle was then pressurized with 10 bar of H_2 and stirred at room temperature. Samples were taken at regular time intervals and analyzed by GC-MS.

Characterization:

^{1}H NMR spectroscopic measurements were carried out by using concentrated solutions of the nanoparticles in $CDCl_3$ with a Bruker 400 MHz NMR spectrometer. X-ray photoelectron spectra (XPS) were performed on a PHI 5400 instrument. Photoluminescence were examined with a Horiba spectrometer. FTIR measurements were carried out with a Nicolet FTIR spectrometer while in-situ FTIR spectra were acquired with an MCT detector cooled with liquid nitrogen. All the IR samples were prepared by spreading the particle solutions onto a ZnSe disk.

Thermogravimetric analysis (TGA) was performed with a Pyris-8000 (Perkin Elmer) instrument at a heating rate of 10℃ min^{-1} under a nitrogen atmosphere. Ru NPs catalysts were dispersed in

15 mL aqua regia (HNO_3/HCl) for 3 h at 150 °C, assisted by microwave technology (2450 MHz), to dissolve Ru NPs completely. Then, the resulting solutions were analysed by inductively coupled plasma optical emission spectroscopy (ICP-OES, Agilent Varian 720) to get the Ru contents.

TG-GC-MS was conducted with an instrument from Perkin Elmer, Pyris8000-Clarus680-ClarusSQ8C with transfer mode of TL9000. **GC test condition:** The GC used manual injection style, with inlet temperature of 280 °C. The ion source temperature was also set at 280 °C. Argon (purity 99.9995%) was used as carrier gas. The gas flow rate through the column was 1 mL/min and the column temperature was held at 280 °C for 134 minutes. The GSV valve was opened for 2 minutes. **MS test condition:** Solvent delay was 4 minutes, and scan range was 35-1000 amu (atomic mass unit) from 5 to 134 minutes. **TG test condition:** The TG test was performed from 30 to 700 °C at 5 °C/min in a helium atmosphere (purity 99.9995%), and the total heating time was 134 minutes.

Table S1. Comparison of the transition temperature for EHB, BEHB, DEHB and the Ru@EHB, Ru@BEHB, Ru@DEHB nanoparticles. s: shoulder

	EHB	Ru@EHB	BEHB	Ru@BEHB	DEHB	Ru@DEHB
T_g (°C)	195.6	271	160.7	264	152.2	277
			300.5	-	300.5	314.3 (s)
				439.1	495.6	474.1

Table S2. The evolution of the hydrogenation product of styrene catalyzed by Ru@EHB, Ru@BEHB and Ru@DEHB nanoparticles respectively

RuNPs	Reaction time (h)								
	0	0.5	1	2	3	4	5	6	18
Ru@EHB	100:0:0	40:60:0	16:84:0	0:77:23	0:10:90	0:0:100	0:0:100	0:0:100	0:0:100
Ru@BEHB	100:0:0	73.4:26.2:0.4	22:78:1	14.8:83.8:1.4	0.7:97.7:1.6	0:97:3	0:95.4:4.6	0:93.7:6.3	0:90.3:9.7
Ru@DEHB	100:0:0	67:33:0	6:94:0	0:99:1	0:97:3	0:96:4	0:95:5	0:95:5	0:93:7
Ru@HC12	100:0:0	99.2:0.8:0	11.6:88.4:0	0:97.3:2.7	0:95.6:4.4	0:90.4:9.6	0:79.6:20.4	0:63.6:36.4	0:21.3:78.7
Ru@PTiol	100:0:0	98.9: 6.1:0	82.2: 17.8:0	65.5: 34.5:0	52.4:47.6:0	38.5:61.5:0	35.7:64.3:0	32.7:67.3:0	0.3:99.7:0:

Products ration in % to a:b:c (a = styrene; b = ethylbenzene; c=ethylcyclohexane). Catalytic condition: T_a = 25 °C; Ru_s/styrene ~ 1 : 300; Ru_s ~ 0.05mmol; H_2 Pressure = 1 MPa. Reaction product was determined by GC-MS

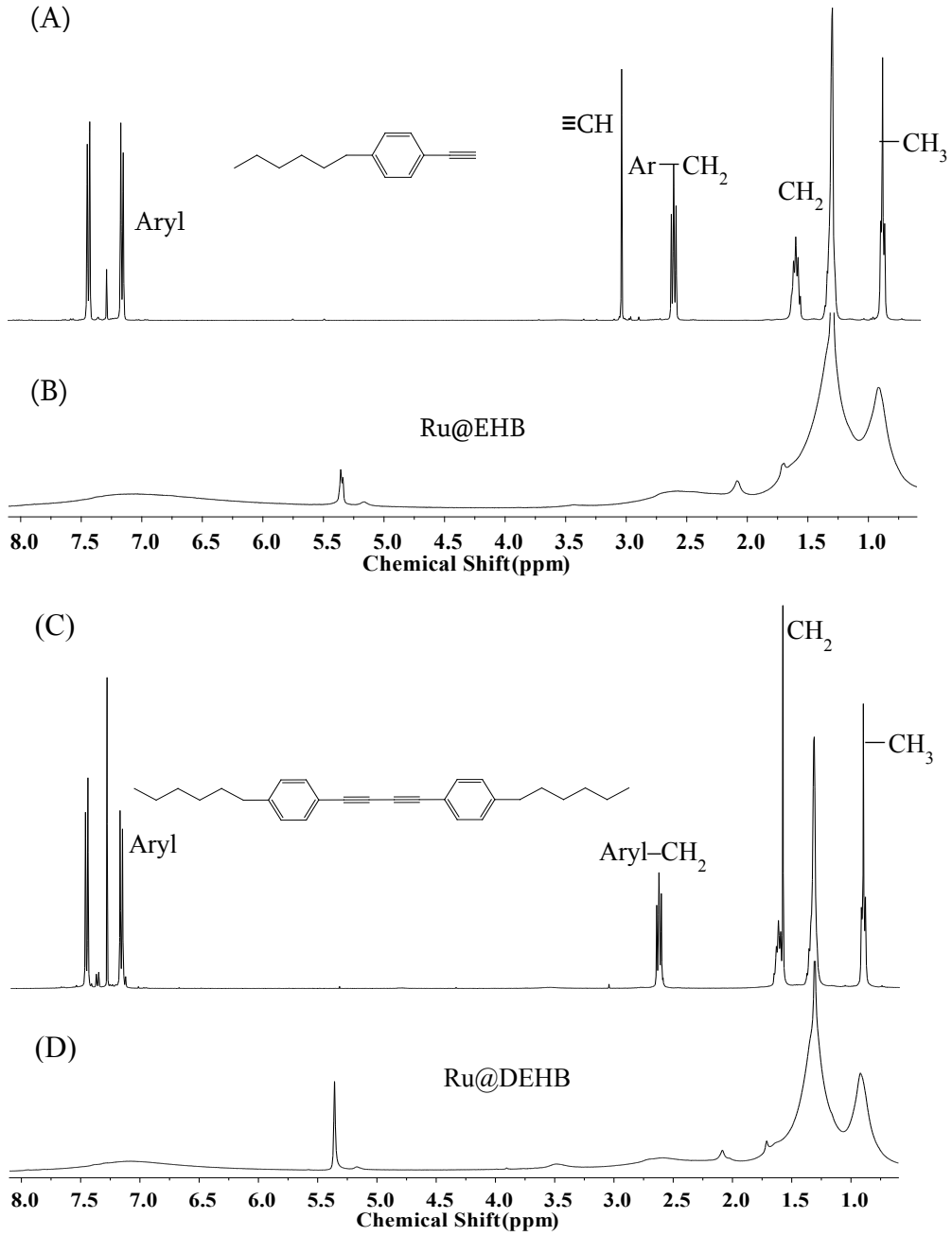
(A)
≡CH
Ar–CH2
CH2
CH3
Aryl
(B)
Ru@EHB
8.0 7.5 7.0 6.5 6.0 5.5 5.0 4.5 4.0 3.5 3.0 2.5 2.0 1.5 1.0
Chemical Shift(ppm)
(C)
CH2
CH3
Aryl
Aryl–CH2
(D)
Ru@DEHB
8.0 7.5 7.0 6.5 6.0 5.5 5.0 4.5 4.0 3.5 3.0 2.5 2.0 1.5 1.0
Chemical Shift(ppm)

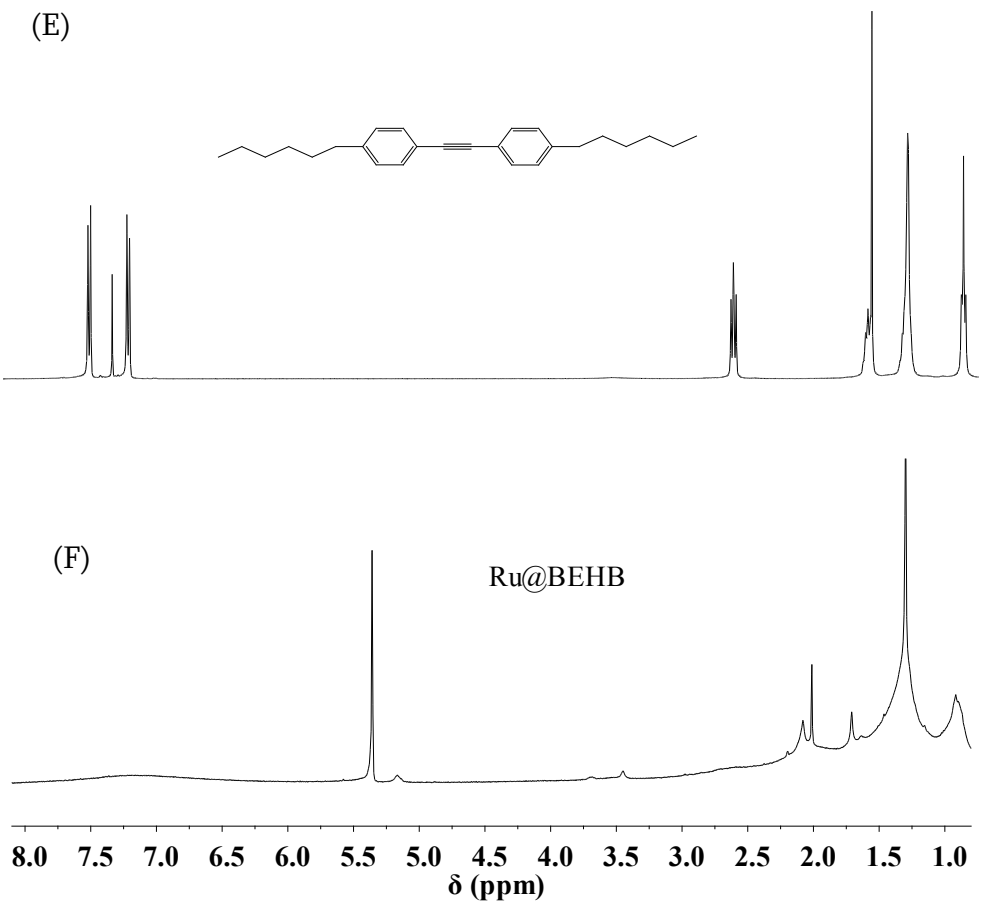

Figure S1. The ^{1}H NMR spcetra of (A) EHB, (B) Ru@EHB, (C) DEHB, (D)Ru@DEHB, (E) BEHB, (F)Ru@BEHB respectively.

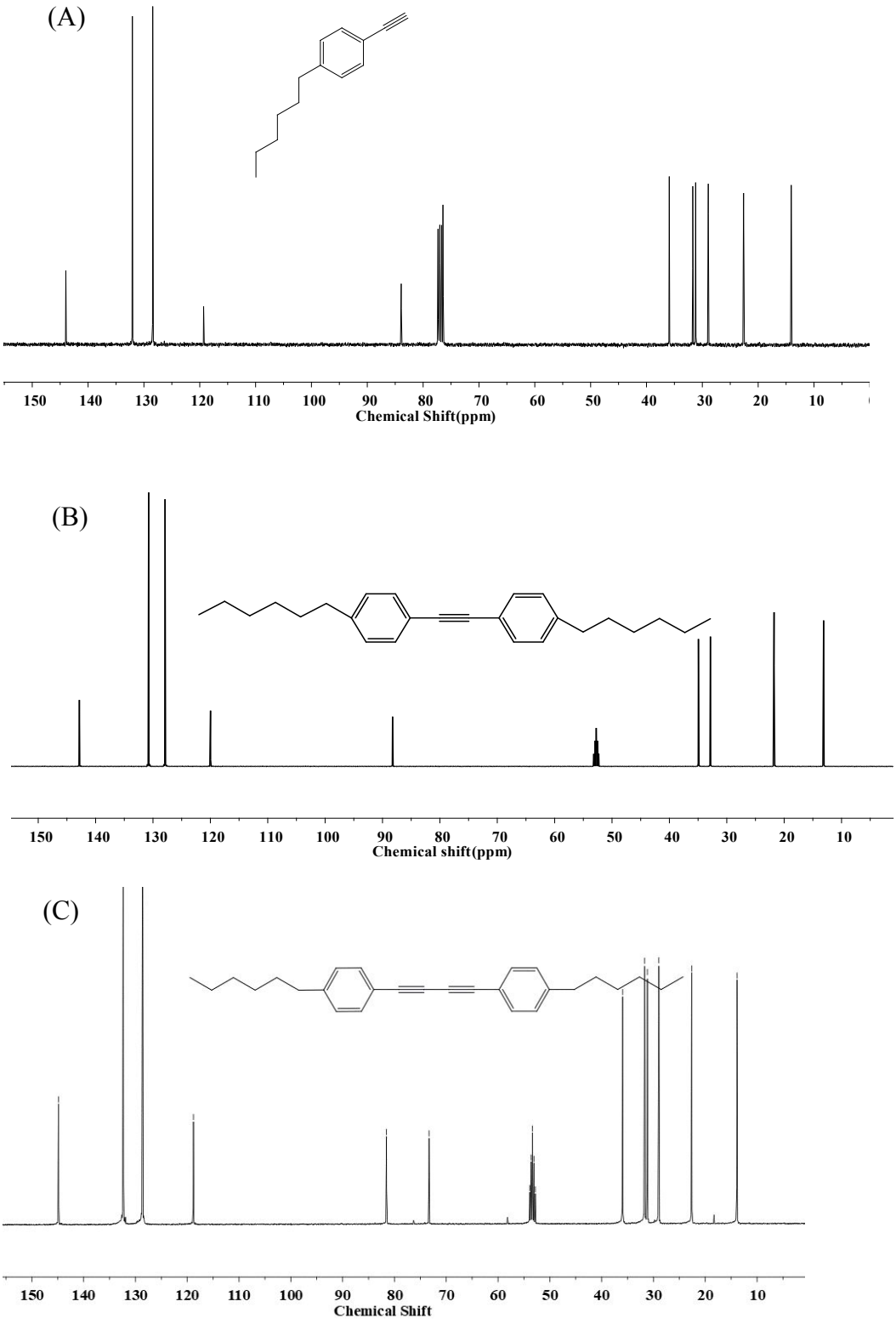

Figure S2. The ^{13}C NMR spectra of (A) EHB, (B) BEHB and (C) DEHB in CD_2Cl_2.

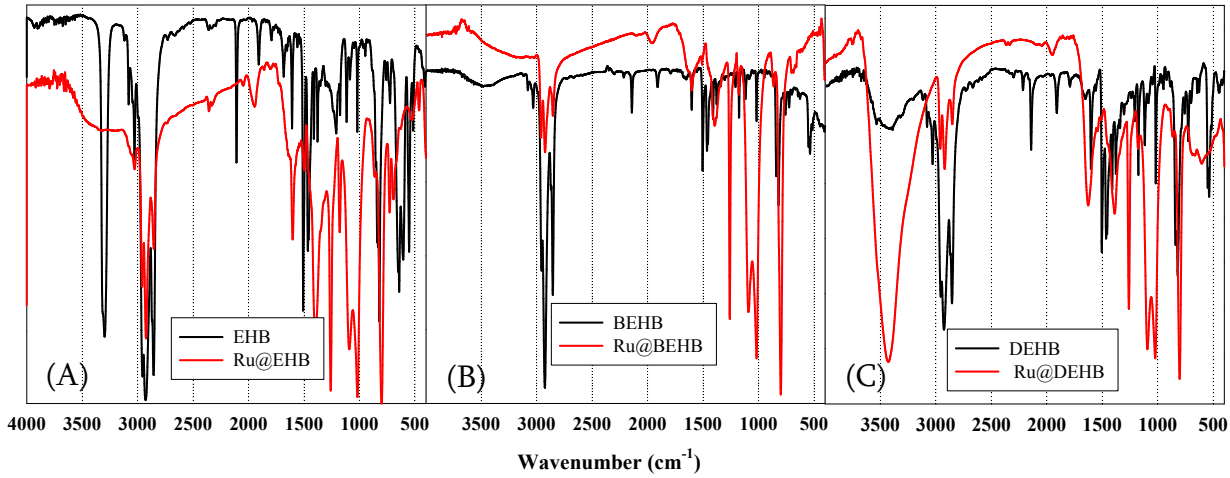

Figure S3. FTIR spectra of (A) EHB and Ru@EHB; (B) BEHB and Ru@BEHB; (C) DEHB and Ru@DEHB nanoparticles.

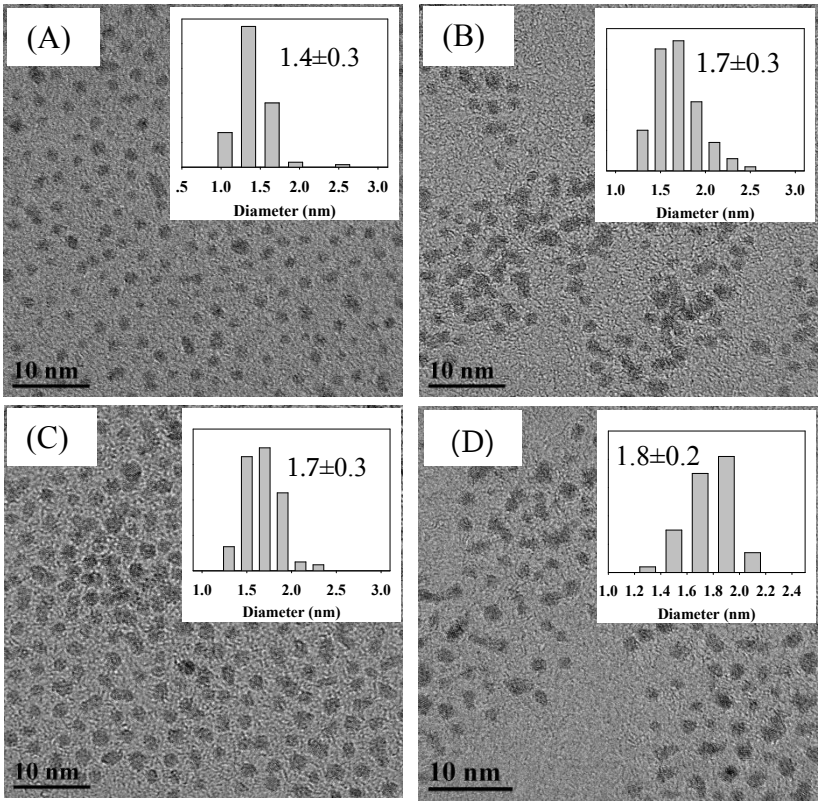

Figure S4. Representative TEM images of (A) Ru@EHB, (B) Ru@BEHB, (C) Ru@DEHB and (D) Ru@DEHB after catalysis. The insets show the histograms of the size distribution of Ru nanoparticles. Scale bar is 10 nm.

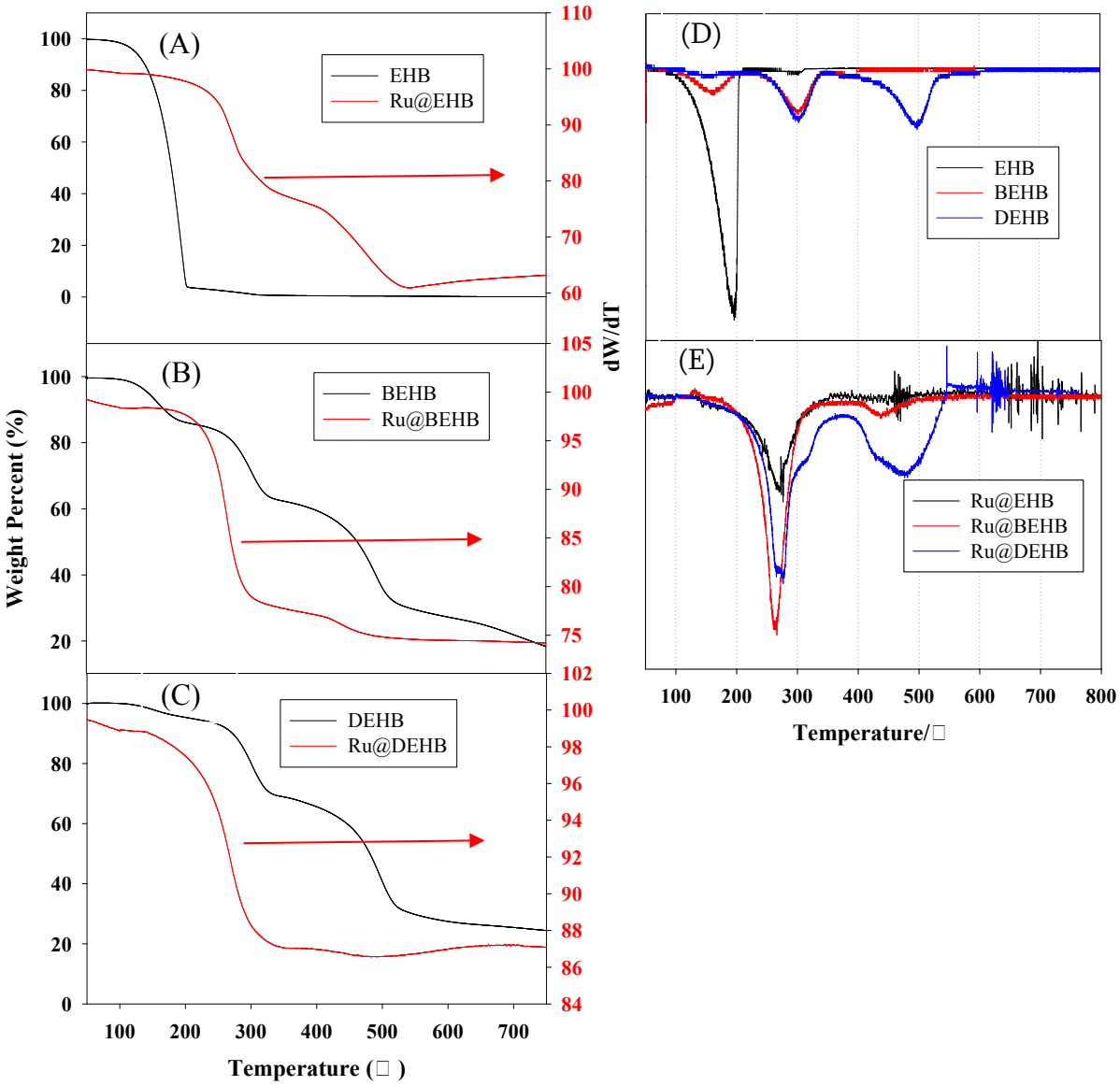

Figure S5. TGA profiles of (A) EHB and Ru@EHB, (B) BEHB and Ru@BEHB, (C) DEHB and Ru@DEHB, first order derivatives of (D) EHB, BEHB and DEHB and (E) Ru@EHB, Ru@DEHB and Ru@BEHB nanoparticles. The black curves (monomers) in (A), (B) and (C) corresponds to the left axis while the red curves (Ru nanoparticles) to right axis.

DFT calculation methods and details

The calculations in this study were performed using the plane-wave pseudopotential method in the framework of DFT.[4] The transition states (TS) were searched by means of complete LST/QST method for each elementary reaction, starting from reactants to products. The ion core and valence electron interaction was described by Vanderbilt-type ultrasoft pseudopotential. The exchange-correlation interactions were treated by the generalized-gradient approximation (PBE/GGA) scheme.[5] The kinetic energy cutoff was set to 300 eV. The convergence thresholds between optimization cycles for energy change and maximum force were set as 10^{-5} eV/atom and 0.03 eV/Å, respectively. The Ru(0001) surface was modeled using a 3-layers slab with a *p*(7×7) unit cells (147 Ru atoms). Since the slab model is large, only the top layer was allowed to relax during the optimization and only a single k-point at (0,0,0) was used for slab optimization. The calculation methods and settings have been verified by the previous study.[6] For the considered system, the van der Waals (vdW) interfaction is crucial for the formation and stability of the interface. The Tkatchenko-Scheffler scheme[7] was adopted to the dispersion correlations.

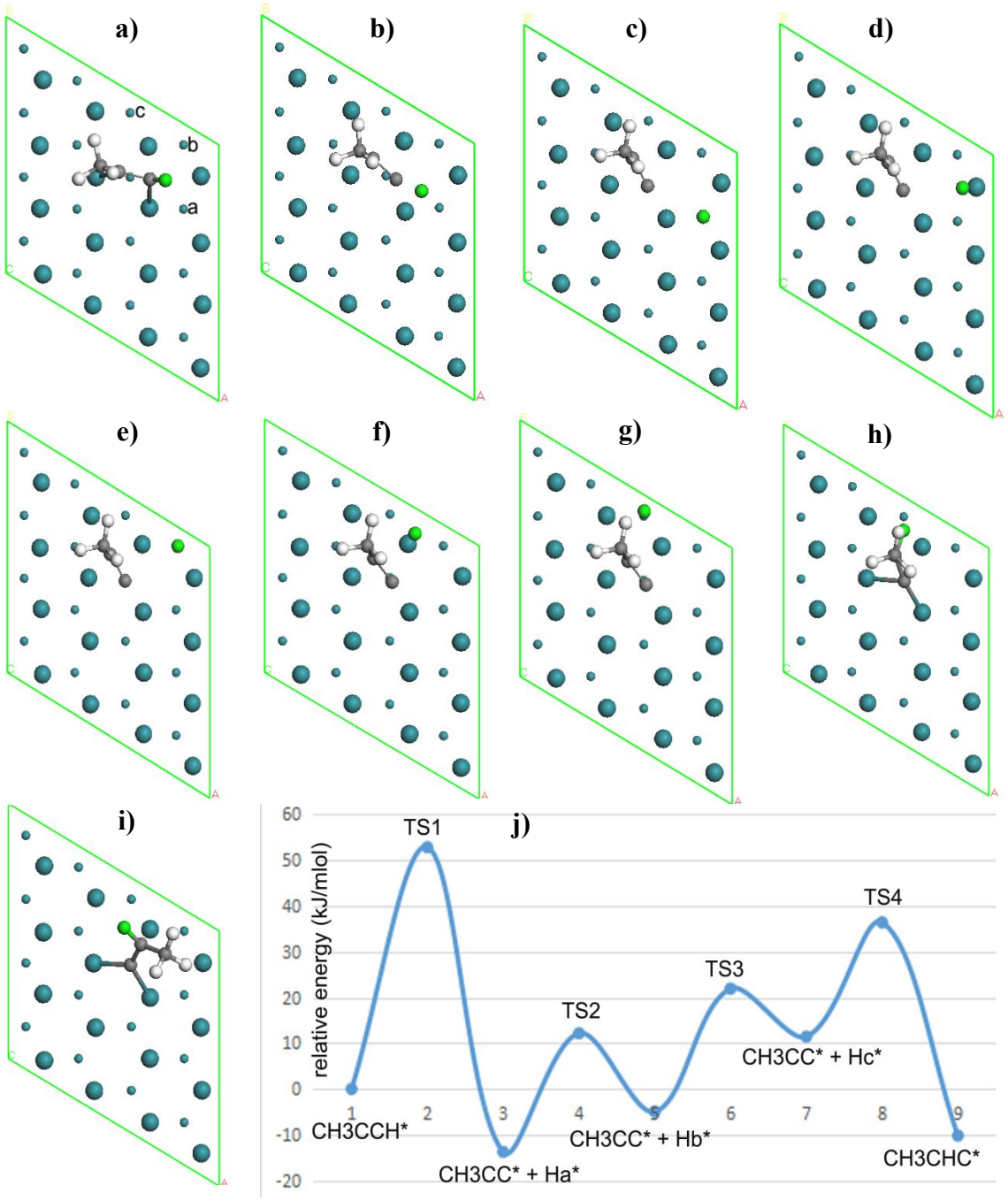

Figure S6. Theoretical calculation of transition states from the adsorbed terminal alkyne to vinylidene. The configuration in panel **a)** to **i)** represents the transition state of **1** to **9** in panel **j)** and panel **j)** shows the energy diagram of each transition state shown in panel **a)** to **i)** during the transition from the adsorbed terminal alkyne to adsorbed vinylidene. The solid grey, dark white and dark green balls represents carbon, hydrogen and ruthenium atoms. The

adsorption energy of 1-propyne on Ru (0001) is 323kJ/mol, much higher than all these energy barriers.

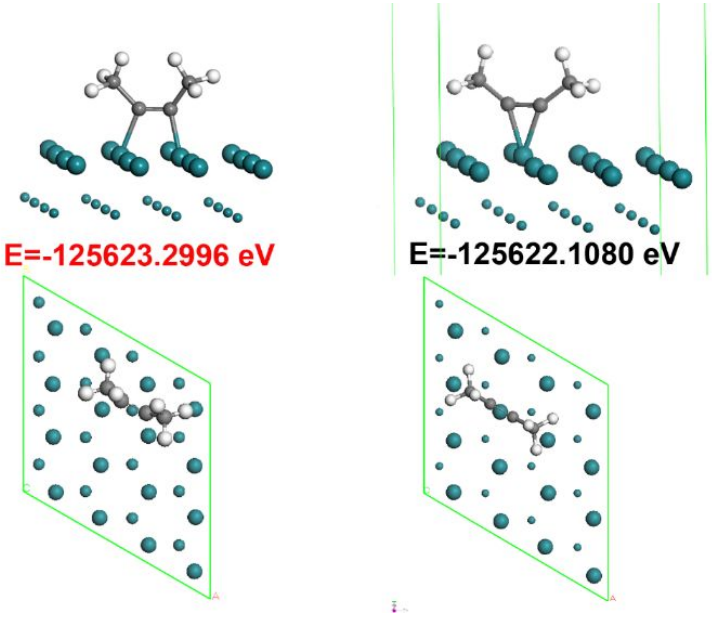

Figure S7. The adsorption configuration of **internal alkyne** CH_3–C≡C–CH_3 on Ru(0001) surface. The internal alkyne prefers to take the bridging site, instead of top site.

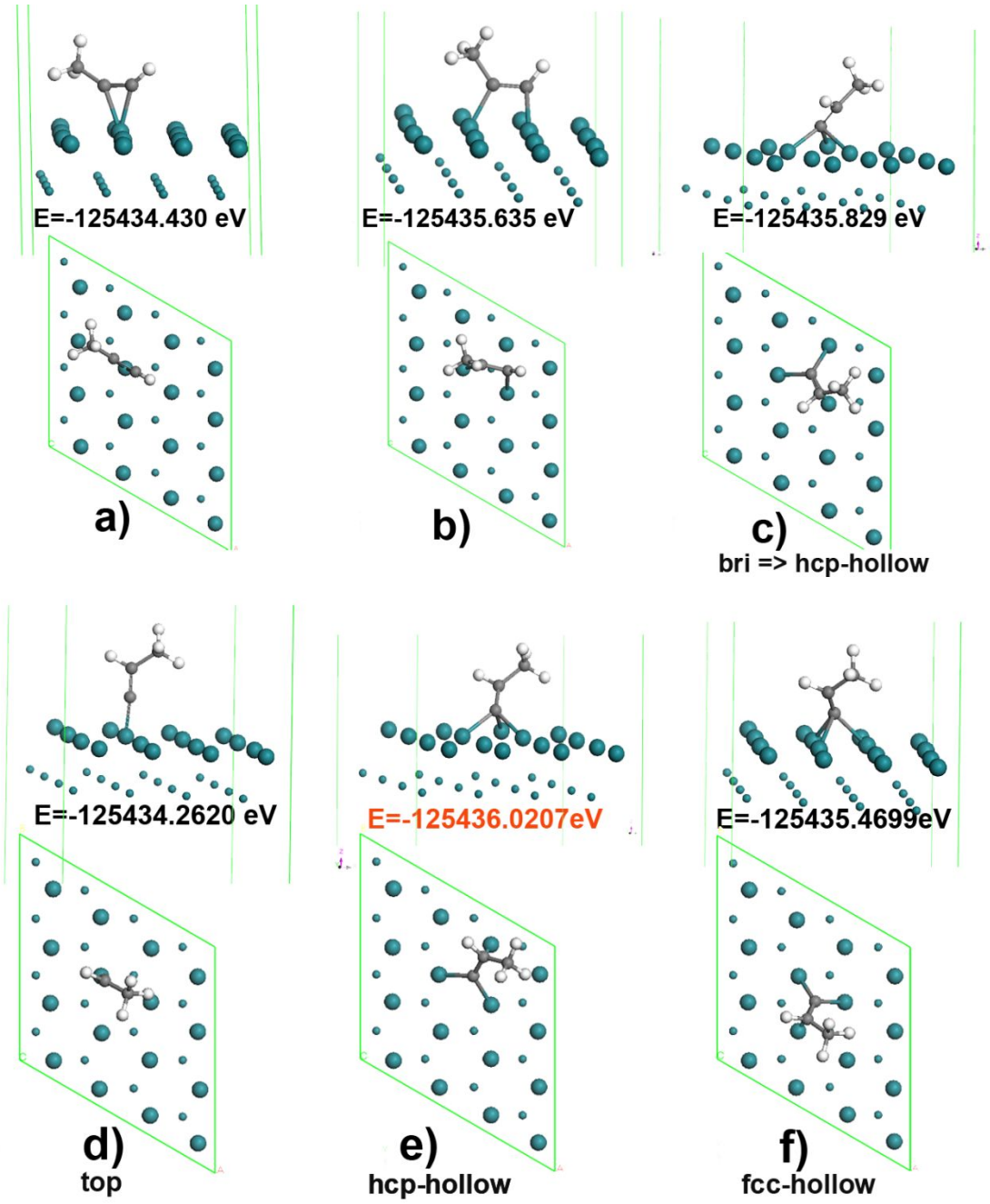

Figure S8. Adsorption configurations of terminal alkyne CH_3–C≡CH on a) top site and b) bridging site of Ru (0001). The adsorption of terminal alkyne on c) hcp-hollow site was derived from the initial state on bridging site, d) top site. Terminal alkyne on e) hcp-hollow and f) fcc-hollow site from the initial state on hcp- and fcc- hollow site. The energy of configuration in c) and e) are very close to each other.

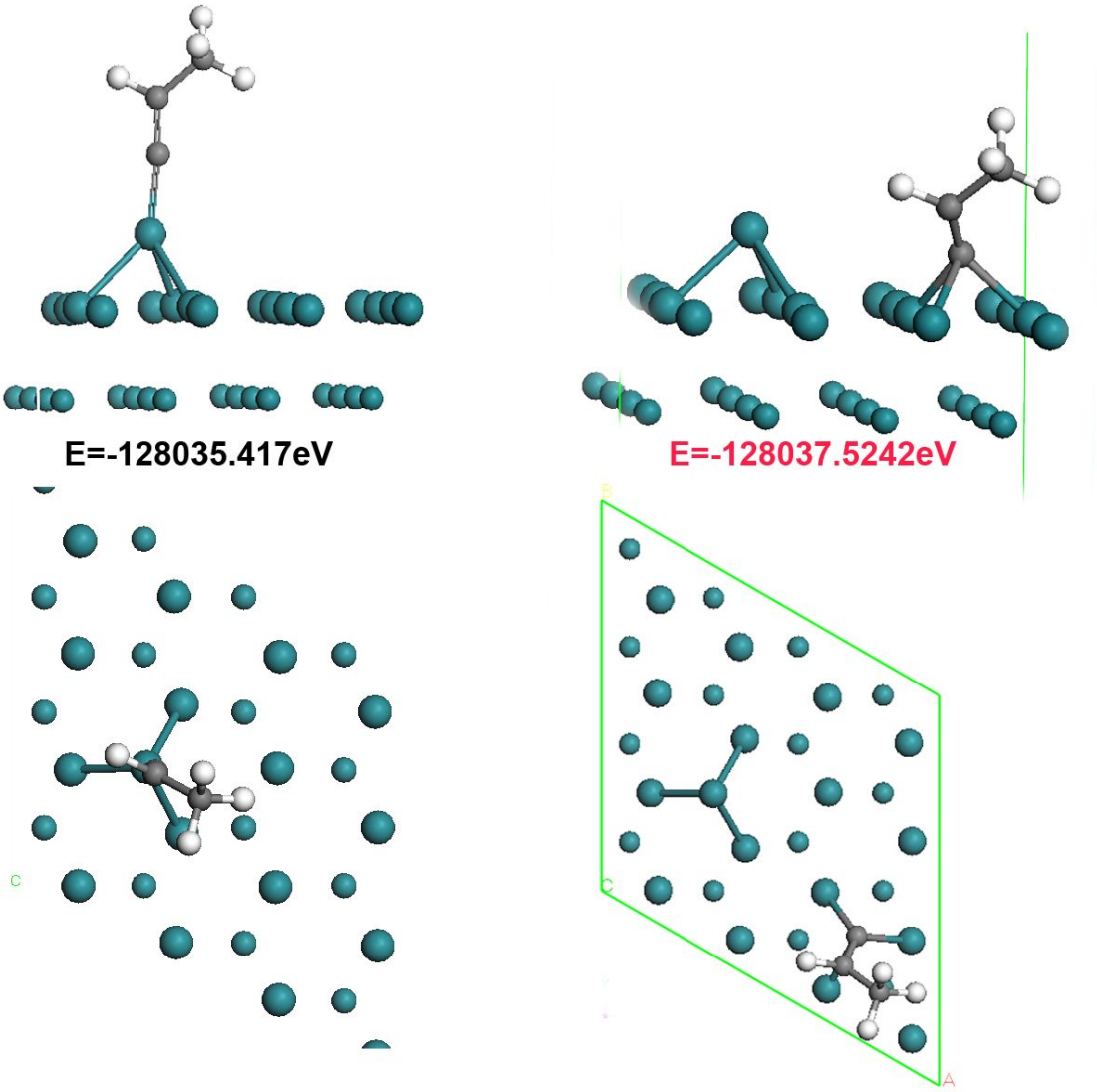

Figure S9. The adsorption configuration of vinylidene CH_3–CH=C= on a) vertex and b) hollow site of Ru (0001) containing vertex structure. It was found that the vinylidene CH_3–CH=C= on hollow site is more preferred than the vertex site.

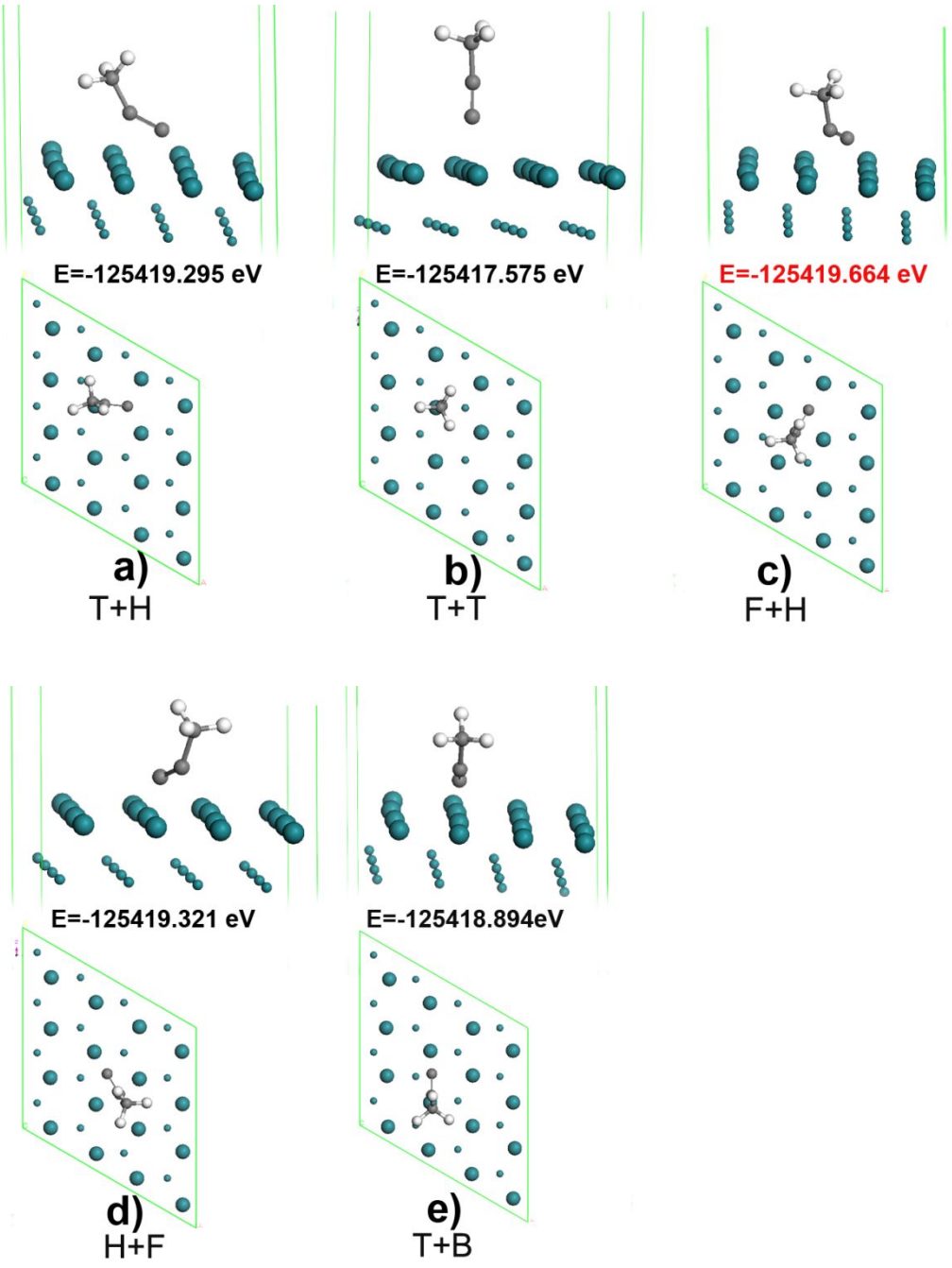

Figure S10. The adsorption configurations of transition state CH_3–C≡C– obtained in Figure S6c) on Ru surfaces. Here F, H, T and B represents the fcc-hollow, the hcp hollow, the top site and the bridging site respectively.

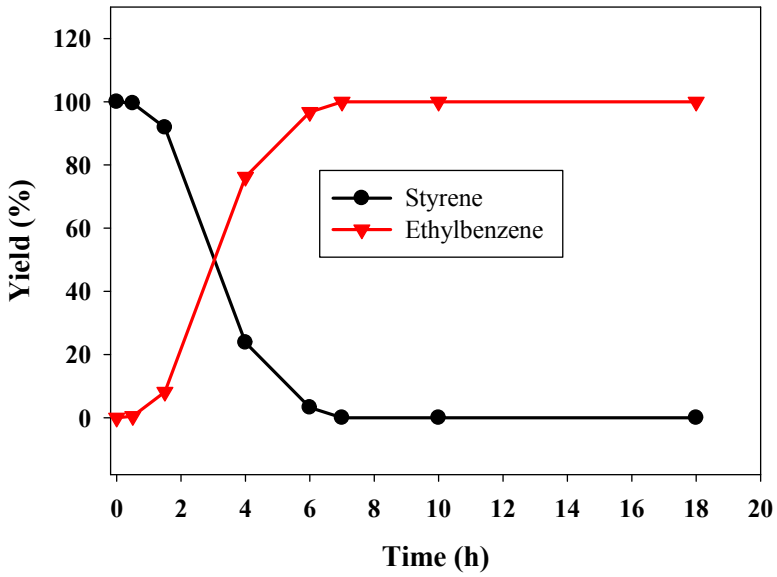

Figure S11. The evolution of hydrogenation products of styrene by CO-poisoned Ru@DEHB nanoparticles.

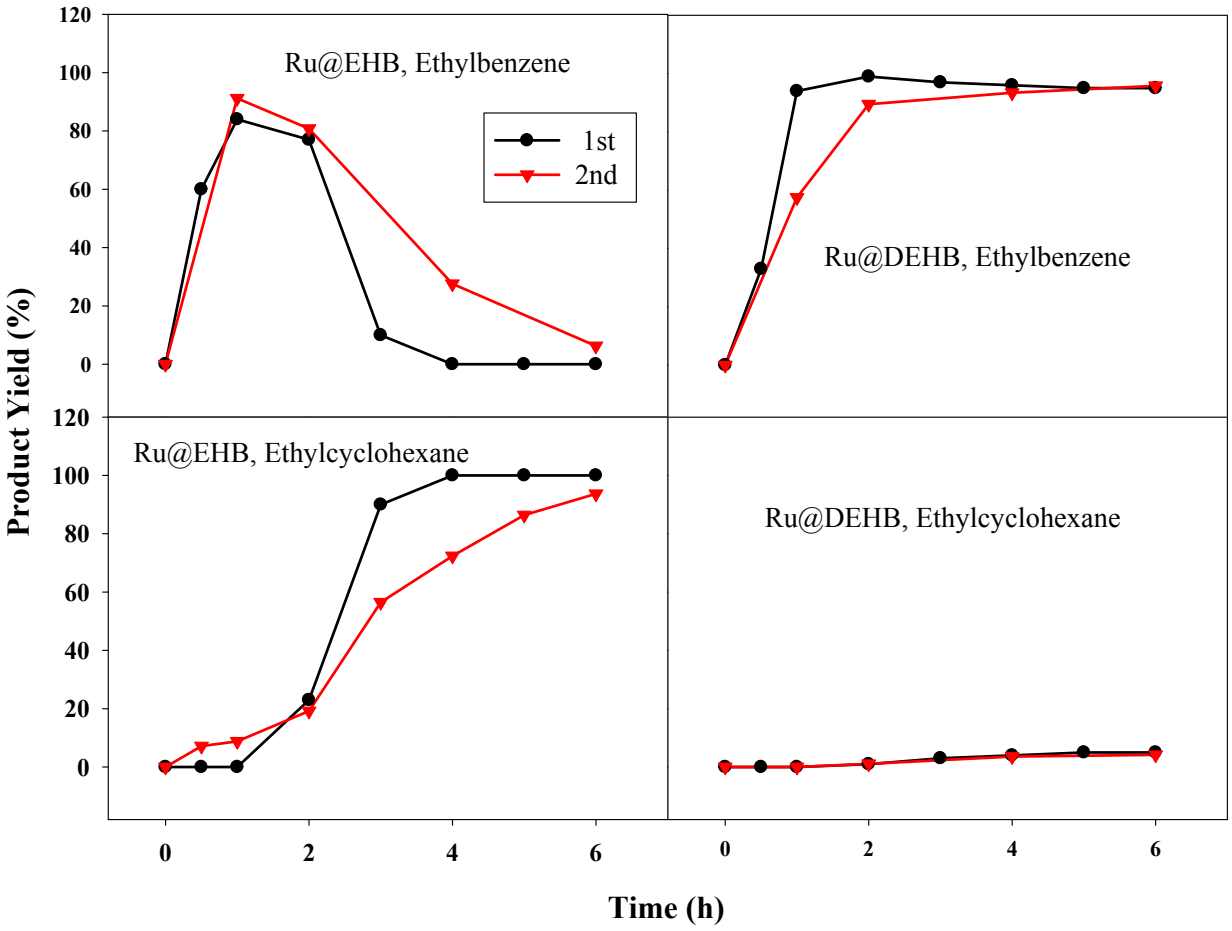

Figure S12. The evolution of hydrogenation products of styrene in the 1st and 2nd test by Ru@EHB and Ru@DEHB nanoparticles.

References

1. Uptmoor, A. C.; Freudenberg, J.; Schwabel, S. T.; Paulus, F.; Rominger, F.; Hinkel, F.; Bunz, U. H. F., Reverse Engineering of Conjugated Microporous Polymers: Defect Structures of Tetrakis(4-ethynylphenyl)stannane Networks. *Angew. Chem. Int. Edit.* **2015,** *54*, 14673-14676.
2. Thorand, S.; Krause, N., Improved Procedures for the Palladium-Catalyzed Coupling of Terminal Alkynes with Aryl Bromides (Sonogashira coupling). *J. Org. Chem.* **1998,** *63*, 8551-8553.
3. Kang, X. W.; Chen, S. W., Electronic Conductivity of Alkyne-Capped Ruthenium Nanoparticles. *Nanoscale* **2012,** *4*, 4183-4189.
4. Clark Stewart, J.; Segall Matthew, D.; Pickard Chris, J.; Hasnip Phil, J.; Probert Matt, I. J.; Refson, K.; Payne Mike, C., First Principles Methods Using CASTEP. In *Zeitschrift für Kristallographie*, 2005, 220, 567.
5. Vanderbilt, D., Soft Self-Consistent Pseudopotentials in a Generalized Eigenvalue Formalism. *Phys. Rev. B* **1990,** *41*, 7892-7895.
6. Mao, J. J.; Chen, W. X.; Sun, W. M.; Chen, Z.; Pei, J. J.; He, D. S.; Lv, C. L.; Wang, D. S.; Li, Y. D., Rational Control of the Selectivity of a Ruthenium Catalyst for Hydrogenation of 4-Nitrostyrene by Strain Regulation. *Angew. Chem. Int. Edit.* **2017,** *56*, 11971-11975.
7. Tkatchenko, A.; Scheffler, M., Accurate Molecular Van Der Waals Interactions from Ground-State Electron Density and Free-Atom Reference Data. *Phys. Rev. Lett.* **2009,** *102*.